Available online at www.sciencedirect.com

ScienceDirect

Ceramics International 40 (2014) 1105–1110

CERAMICS INTERNATIONAL

www.elsevier.com/locate/ceramint

Decisive role of MgO addition in the ultra-broad temperature stability of multicomponent $BaTiO_3$-based ceramics

Lingxia Li*, Mingjing Wang, Yaran Liu, Junxiao Chen, Ning Zhang

School of Electronic and Information Engineering, Tianjin University, Tianjin 300072, China

Received 1 May 2013; received in revised form 28 June 2013; accepted 28 June 2013
Available online 5 July 2013

Abstract

High capacitance temperature stability (the capacitance is within ±15% of room temperature capacitance) in an ultra-broad temperature range of −55 °C to 300 °C has been achieved by synthesizing multicomponent $BaTiO_3$-based ceramics consisting of $BaTiO_3$, $Na_{0.5}Bi_{0.5}TiO_3$, Nb_2O_5, CeO_2, glass and MgO. Significantly, MgO addition plays a decisive role in achieving the ultra-broad temperature stability and acquiring an appropriate microstructure. Doping different amounts of MgO can alter the temperature dependence of dielectric constant markedly, especially in a high temperature range of 200 °C–300 °C. The maximum capacitance variation rate is reduced from −60% to only 10% by doping appropriate content of MgO. In terms of the microstructure, MgO additive can suppress the formation of Ti-rich phase and sheet grains, which are detrimental to the capacitance temperature stability. The sample with 1.5 wt% MgO has superior dielectric and electrical properties at room temperature (ε_r=1675, tan δ=1.452%, and $\rho_V=5\times10^{12}$ Ω cm).
© 2013 Elsevier Ltd and Techna Group S.r.l. All rights reserved.

Keywords: Dielectrics; Ceramics; $BaTiO_3$; Temperature stability

1. Introduction

High and stable dielectric constants over a broad temperature are significant for $BaTiO_3$-based ceramics, due to their use in multi-layer ceramic capacitors (MLCCs). Electronic Industries Alliance (EIA) X7R and X8R specifications (X7R: from −55 to 125 °C, the capacitance is within ±15% of room temperature capacitance; X8R: from −55 to 150 °C, the capacitance is within ±15% of room temperature capacitance) were established to meet requirements for different applications [1–4]. However, X7R, X8R or even X9R (from −55 to 200 °C, the capacitance is within ±15% of room temperature capacitance) [5–9] materials cannot satisfy the application requirements of MLCCs in harsh conditions, such as oil drilling, aerospace and automotive environment [10–13]. For example, the working temperature in the cylinder is 200–300 °C [10]. So it is of great need to develop ultra-broad temperature stable materials for a wider application. We previously reported that $BaTiO_3$–$Na_{0.5}Bi_{0.5}TiO_3$–Nb_2O_5–MgO-rare earth oxide system acquired X9R characteristics, and found that the multicomponent $BaTiO_3$-based system was promising for the capacitance temperature stability in an ultra-broad temperature range of −55 °C to 300 °C [9,14]. MgO is an important additive in $BaTiO_3$-based ceramics, and many studies have shown that MgO additive can help satisfy X7R and X8R specifications by promoting the core–shell structure or suppressing grain growth [15–19]. While, there is no relative investigations about the effect of MgO on ultra-broad temperature stable ceramics, especially the effect on the dielectric properties in a high temperature range of 200 °C–300 °C.

In this study, we prepared multicomponent $BaTiO_3$-based ceramics to achieve the ultra-broad temperature stability (from −55 to 300 °C, the capacitance is within ±15% of room temperature capacitance). Furthermore, we investigated the effects of different MgO contents on the dielectric properties and microstructure of multicomponent $BaTiO_3$-based ceramics, and discussed the decisive role of MgO addition in achieving the ultra-broad temperature stability.

2. Experimental procedures

The experimental procedure of multicomponent $BaTiO_3$-based ceramics is depicted in Fig. 1. The purity of starting

*Corresponding author. Tel./fax:+86 22 27402838.
E-mail address: llxtju@126.com (L. Li).

0272-8842/$ - see front matter © 2013 Elsevier Ltd and Techna Group S.r.l. All rights reserved.
http://dx.doi.org/10.1016/j.ceramint.2013.06.110

materials is higher than 99%. $Na_{0.5}Bi_{0.5}TiO_3$ (NBT) powders were synthesized by using reagent-grade oxide or carbonate powders of Na_2CO_3, Bi_2O_3 and TiO_2. The starting materials were mixed by ball-milling for 4 h using zirconia milling media in deionized water, followed by drying, then calcined at 800 °C to synthesize NBT. Precursor was composed of $BaTiO_3$ (400 nm average grain size, Guoci Co. Ltd., China), synthesized NBT and Nb_2O_5 powders with the mole ratio of BT:NBT:Nb_2O_5 = 85:15:2. The powders were mixed by ball-milling for 4 h, and then calcined at 1000 °C for 2 h. The glass powders were synthesized by 23.55 wt% Bi_2O_3, 19.85 wt% TiO_2, 24.30 wt% ZnO and 32.30 wt% B_2O_3. In the final preparation of samples, 25 g precursor, 0.10 g CeO_2, 1.25 g glass powders and various amounts of MgO (0.0, 1.0, 1.5 and 2.0 wt%) were mixed by 2 h ball-milling. After drying, mixed powders were added in 7 wt% binder wax, and then pressed into discs with 20 mm in diameter and 1 mm in thickness. Samples were sintered at 1130 °C for 1 h.

Dielectric loss and capacitance were measured by use of a capacitance meter (HP4278A) at 1 kHz, with temperature range of −55 °C to 300 °C. The capacitance variation rate ($\Delta C/C_{20\,^\circ C}$) is calculated by using the equation $\Delta C/C_{20\,^\circ C} = (C - C_{20\,^\circ C})/C_{20\,^\circ C} \times 100\%$, where $C_{20\,^\circ C}$ is the capacitance at 20 °C, and C is the capacitance of either temperature in the range of −55 °C to 300 °C. The frequency characteristics were measured between 200 Hz and 1 MHz, using a TH2828S automatic component analyzer. Insulation resistance was measured using a high resistance meter (Agilent 4339B) at room temperature. Crystal structure of the samples was identified at room temperature using an X-ray diffractometer (D8-Focus, Bruker AXS GmbH, Germany). Microstructure of the ceramic samples was observed by field emission scanning electron microscopy (FE-SEM, S-4800, Hitachi, Ltd., Japan). Element distribution of different areas was analyzed by energy dispersive spectrometry (EDS).

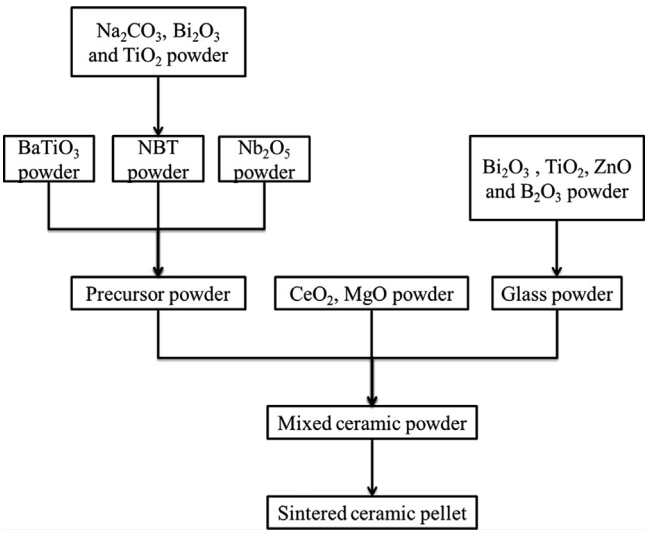

Fig. 1. Flow chart for the fabrication of the multicomponent $BaTiO_3$-based ceramics.

3. Results and discussion

Fig. 2 shows the temperature dependence of dielectric constant for samples with various amounts of MgO. The curve of the sample without MgO presents an obvious dielectric constant peak at about 125 °C, just as pure $BaTiO_3$. For the sample with 1.0 wt% MgO, the peak at 125 °C is suppressed, and meanwhile, the dielectric constant is markedly enhanced at lower temperature. With the continued increasing MgO content, the curve shape changes greatly. In the case of 1.5 wt% and 2.0 wt% MgO, there are two dielectric constant peaks at about −20 °C and 250 °C. The change is beneficial to the improvement of temperature stability, especially in the high-temperature range (150 °C–300 °C). The effect of MgO addition on the temperature stability of samples can be also described well by the temperature dependence of capacitance variation rate, as shown in Fig. 3. For the sample with 0.0 wt% and 1.0 wt% MgO, the capacitance variation rate is relatively large in the high-temperature range (150 °C–300 °C). The maximum capacitance variation rate of the sample with 1.0 wt% MgO is even up to −60%. When MgO doping content reaches to 1.5 wt%, the temperature stability is improved dramatically, especially in the high-temperature range. The maximum capacitance variation rate is down to only about 10%, which can satisfy the ultra-broad temperature stability specification well. While, the capacitance variation rate is beyond 15% in the temperature from 200 °C to 300 °C for the sample with 2.0 wt% MgO. Therefore, appropriate amount of MgO addition enables $BaTiO_3$-based ceramics to satisfy the ultra-broad temperature stability. The dielectric loss curves of different samples over the broad temperature range of −55 C to 300 °C are shown in Fig. 4. Dielectric loss data of samples with 1.5 wt% and 2.0 wt% MgO differ from those of samples with 0.0 wt% and 1.0 wt% MgO. The curves of samples with 0.0 wt% and 1.0 wt% MgO are relatively flat; while, a distinct dielectric loss peak around 200 °C is observed in the samples with 1.5 wt% and 2.0 wt% MgO. Leakage conductivity has an important effect on dielectric loss in high temperature [6]. In our multicomponent system, the leakage conductivity is supposed to be produced by migration of oxygen vacancies [20]. Zhang et al. reported that

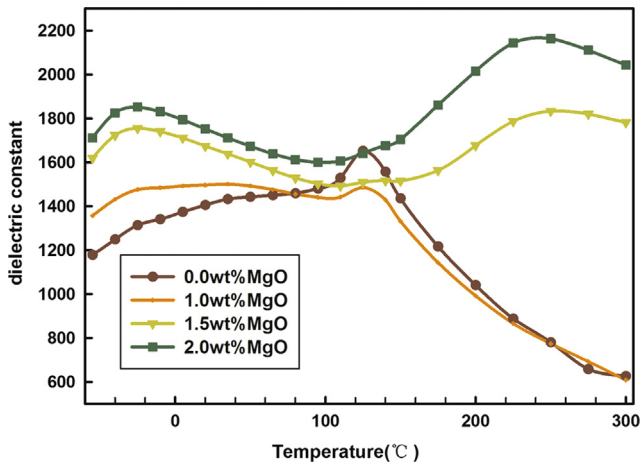

Fig. 2. Temperature dependence of dielectric constant for samples with various amounts of MgO.

Ca-doped $BaTiO_3$ had higher grain conductivity at modest temperatures compared to undoped $BaTiO_3$ ceramics and significantly lower activation energies associated with the bulk conduction mechanism, ~0.4–0.6 eV compared to ~1.40 eV for undoped $BaTiO_3$ [21]. Accordingly, it is speculated that the incorporation of Mg will also have a profound effect on bulk conduction mechanism, i.e., lowering the activation energy.

Insulation resistivity of samples with different Mg doping contents is shown in Table 1. Insulation resistivity decreases gradually with the increasing of Mg doping, which means that the incorporation of Mg increase the conductivity of samples. It is reasonable to predict that the conductivity of samples with Mg doping will increase with increasing temperature because high temperature will promote the motion of oxygen vacancies.

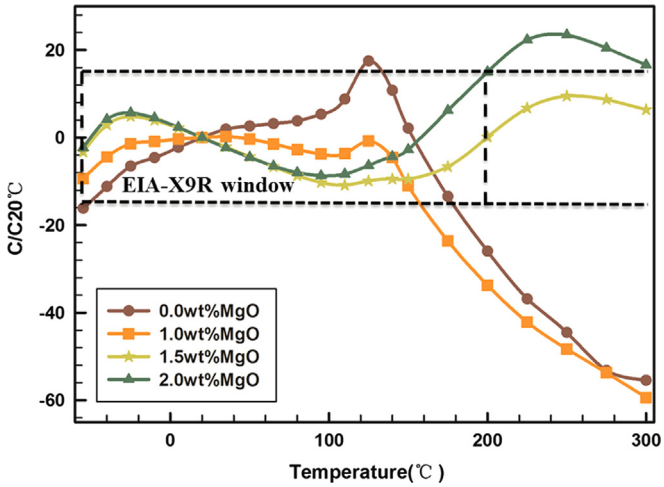

Fig. 3. Temperature dependence of capacitance variation rate based on $C_{20\ ^\circ C}$ for samples with various amounts of MgO.

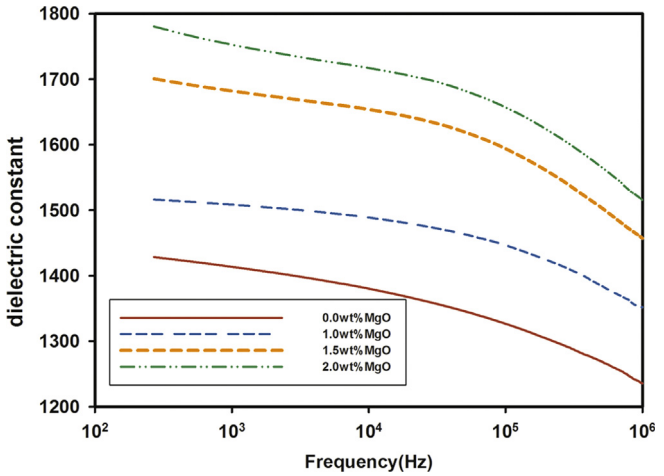

Fig. 5. Frequency dependence of dielectric constant for samples with various amounts of MgO.

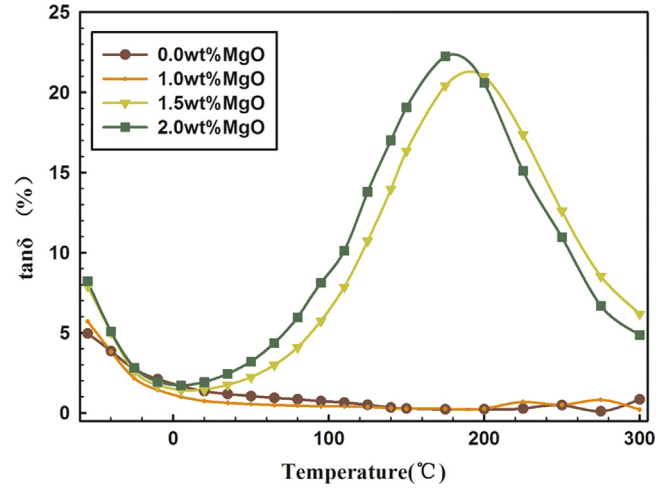

Fig. 4. Temperature dependence of dielectric loss for samples with various amounts of MgO.

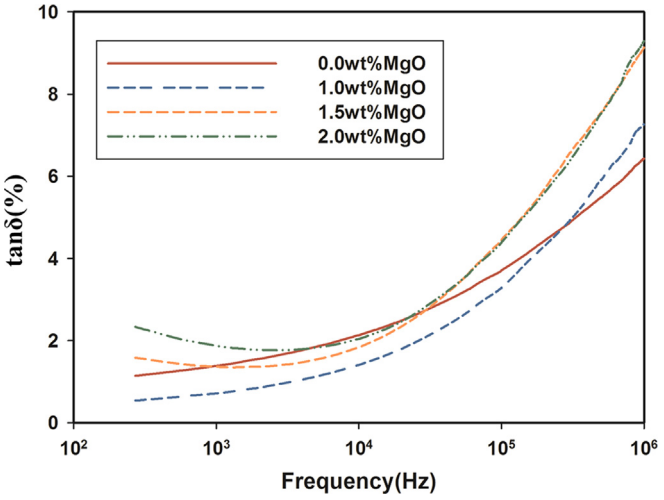

Fig. 6. Frequency dependence of dielectric loss for samples with various amounts of MgO.

Table 1
Dielectric and electrical properties of the samples.

MgO content (mol%)	ε_r at 20 °C	tan δ at 20 °C (%)	$\Delta C/C_{20\ ^\circ C}$ (%)		Insulation resistivity (10^{13} Ω cm)
			−55 °C	300 °C	
0.0	1405	1.354	−16.1	−55.4	6.1
1.0	1497	0.743	−9.4	−59.4	1.8
1.5	1675	1.452	−3.3	6.4	0.5
2.0	1753	1.929	−2.3	16.6	0.4

The dependence of dielectric constant on frequency is shown in Fig. 5. The dielectric constant increases with increasing MgO content in the frequency range from 200 Hz to 1 MHz. For the samples with different amounts of MgO, the variation of dielectric constant with frequency is similar: dielectric constant decreases gradually with increasing frequency. The higher dielectric constant at lower frequencies is due to the contribution of all different types of polarizations (i.e. electronic, ionic, dipolar, interfacial, etc.) [22]. While, only electronic and ionic polarization is dominated at higher frequencies. Fig. 6 shows the dependence of dielectric loss on frequency. The values of samples with 0.0 wt% and 1.0 wt% MgO increase with increasing frequency; while, the values of samples with 1.5 wt% and 2.0 wt% MgO decrease first and then increase with increasing frequency.

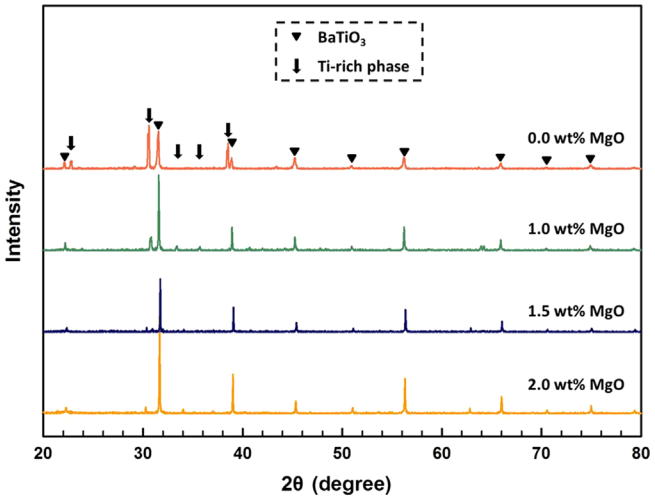

Fig. 7. XRD patterns of samples with various amounts of MgO.

Main dielectric and electrical properties of the samples are listed in Table 1. Dielectric constant at 20 °C increases with the increase of MgO content. Dielectric loss at 20 °C is all lower than 2.0%. With increasing MgO content, the dielectric loss (tan δ) at 20 °C decreases first, and then increases. Besides, samples have superior insulation resistivity ($>10^{12}$ Ω cm), but the insulation resistivity decreases gradually with the increasing of MgO content as discussed above. In brief, the sample with 1.5 wt% MgO is obtained to satisfy the ultra-broad temperature stability. Particularly, the ceiling working temperature has been greatly enhanced from 200 °C to 300 °C. Meanwhile, it has superior dielectric and electrical properties at room temperature: high dielectric constant (1675), low dielectric loss (1.452%) and high insulation resistivity (5×10^{12} Ω cm).

Fig. 7 shows XRD patterns of the multicomponent $BaTiO_3$-based ceramics with different amounts of MgO. As discussed above, the sample with 1.5 wt% MgO obtains the optimum performance. Compared with its pattern, there is a much more noticeable Ti-rich phase in the pattern of the sample without MgO, such as $BaO(TiO_2)_4$. It is found that diffraction peak intensity of the Ti-rich phase decreases perceptibly with the increase of MgO content. In particular, the Ti-rich phase is oblivious in the pattern of the sample with 1.5 wt% MgO. Many studies have reported that some additives can react with $BaTiO_3$ to form disparate phases, such as $Ba_4Ti_{13}O_{20}$, $Ba_6Ti_{17}O_{40}$ and $Ba_2TiSi_2O_8$ [23–25]. In our multicomponent $BaTiO_3$-based ceramics, the Ti-rich phase was formed via the reaction of excess TiO_2 with $BaTiO_3$. To associate with the dielectric properties above, the Ti-rich phase is detrimental to the capacitance temperature stability, especially in the high-temperature range. It is an appropriate amount (1.5 wt%) of MgO addition that suppresses the Ti-rich phase effectively and improves the temperature stability.

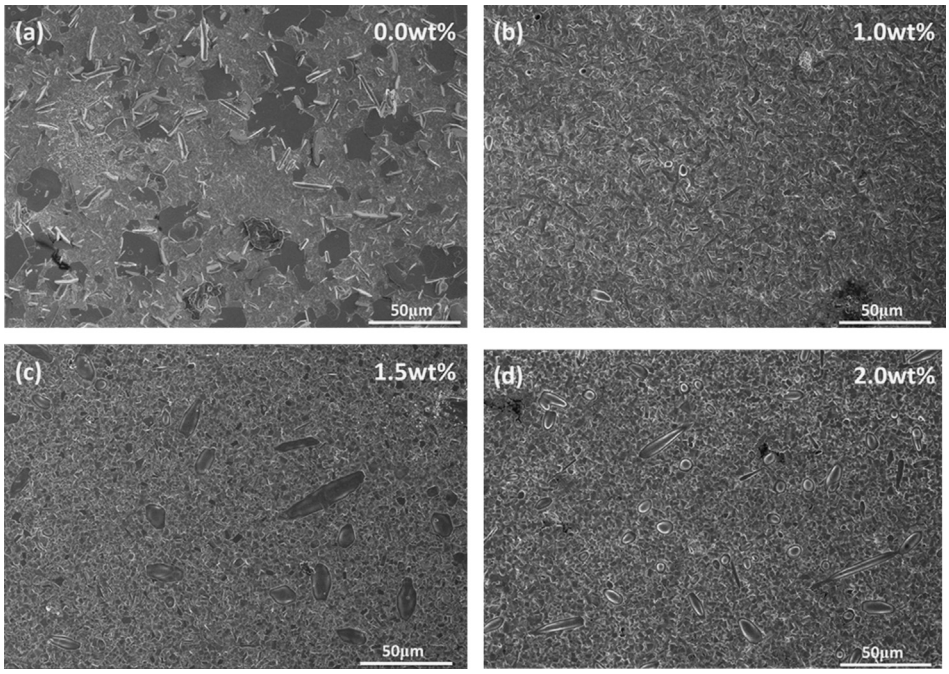

Fig. 8. SEM photos of samples with various amounts of MgO: (a) 0.0 wt%; (b) 1.0 wt%; (c) 1.5 wt%; and (d) 2.0 wt%.

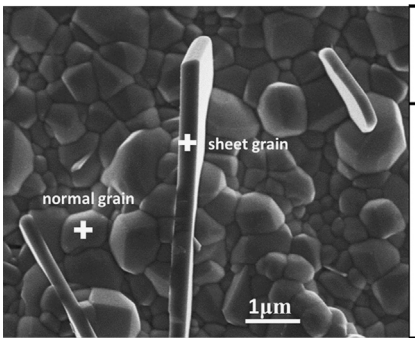

Element	Atomic percentage (%)	
	Normal grain	Sheet grain
Ba-L	21.15	12.36
Ti-K	24.37	33.12
O-K	47.46	51.51
Na-K	2.59	——
Bi-M	1.81	——
Zn-K	2.62	3.01

Fig. 9. Element distribution of two kinds of grains in the sample without MgO.

SEM images of samples with different amounts of MgO are shown in Fig. 8. There are a lot of sheet grains in the sample without MgO. However, with the increasing content of MgO, the sheet grains reduce drastically and even disappear in the sample with 1.5 wt% and 2.0 wt% MgO. To confirm the element distribution in different grains, EDS analysis was carried out and the result is given in Fig. 9. In normal grains, Ti/Ba ratio is about 1. While, in sheet grains, Ti/Ba ratio is approximately 3. It can be considered that the sheet grains are mainly consisting of the Ti-rich phase, as mentioned in the discussion of XRD patterns. The results fit well with the change in XRD patterns. Likewise, sheet grains are detrimental to the ultra-broad temperature stability, and appropriate MgO content can suppress the formation of sheet grains effectively.

4. Conclusions

Multicomponent $BaTiO_3$-based ceramics consisting of $BaTiO_3$, $Na_{0.5}Bi_{0.5}TiO_3$, Nb_2O_5, CeO_2, glass and MgO were synthetized and investigated. In the system, MgO addition plays a decisive role in achieving the ultra-broad temperature stability and acquiring an appropriate microstructure. MgO additive can alter the curve shape of temperature dependence of dielectric constant greatly: from curves with one dielectric peak at 125°C to curves with two dielectric peaks at −20 °C and 250 °C. Capacitance temperature stability is improved effectively: maximum capacitance variation rate is reduced from −60% to only 10%. Sample with 1.5 wt% MgO has the optimum performance: the capacitance variation rate based on $C_{20\ ^\circ C}$ is within ±15% in the ultra-broad temperature range of −55 °C to 300 °C; meanwhile, it maintains good dielectric and electrical properties at room temperature-high dielectric constant (1675), low dielectric loss (1.452%) and high insulation resistivity (5×10^{12} Ω cm). Ti-rich phase and sheet grains, which are detrimental to the capacitance temperature stability, reduce dramatically with the increasing content of MgO.

References

[1] L. Li, R. Fu, Q. Liao, L. Ji, Doping behaviors of NiO and Nb_2O_5 in $BaTiO_3$ and dielectric properties of $BaTiO_3$-based X7R ceramics, Ceramics International 38 (2012) 1915–1920.

[2] Y. Sun, H. Liu, H. Hao, S. Zhang, L. Guo, Z. Yu, Effect of $Na_{0.5}Bi_{0.5}TiO_3$ on dielectric properties of $BaTiO_3$ based ceramics, Ceramics International 38 (2012) S41–S44.

[3] L. Li, M. Wang, D. Guo, R. Fu, Q. Meng, Effect of Gd amphoteric substitution on structure and dielectric properties of $BaTiO_3$-based ceramics, Journal of Electroceramics 30 (2013) 129–132.

[4] J. Kim, T. Noh, S. Jeon, S. Park, H. Chun, H. Lee, Deterioration behavior analysis of dysprosium and thulium co-doped barium titanate ceramics for multilayer ceramic capacitors, Ceramics International 38 (2012) 6837–6842.

[5] S. Wang, J. Li, Y. Hsu, Y. Wu, Y. Lai, M. Chen, Dielectric properties and microstructures of non-reducible high-temperature stable X9R ceramics, Journal of the European Ceramic Society 33 (2013) 1793–1799.

[6] G. Yao, X. Wang, Y. Zhang, Z. Shen, L. Li, Nb-modified $0.9BaTiO_3$–$0.1(Bi_{0.5}Na_{0.5})TiO_3$ ceramics for X9R high-temperature dielectrics application prepared by coating method, Journal of the American Ceramic Society 95 (2012) 3525–3531.

[7] B. Tang, S. Zhang, X. Zhou, Y. Yuan, L. Yang, Preparation and modification of high Curie point $BaTiO_3$-based X9R ceramics, Journal of Electroceramics 25 (2010) 93–97.

[8] S. Gao, S. Wu, Y. Zhang, H. Yang, X. Wang, Study on the microstructure and dielectric properties of X9R ceramics based on $BaTiO_3$, Materials Science and Engineeing B: Advanced Functional Solid-State Materials 176 (2011) 68–71.

[9] L. Li, Y. Han, P. Zhang, C. Ming, X. Wei, Synthesis and characterization of $BaTiO_3$-based X9R ceramics, Journal of Materials Science 44 (2009) 5563–5568.

[10] R.W. Johnson, J.L. Evans, P. Jacobsen, J.R. Thompson, M. Christopher, The changing automotive environment: high-temperature electronics, IEEE Transactions on Electronics Packaging Manufacturing 27 (2004) 164–176.

[11] M.R. Werner, W.R. Fahrner, Review on materials, microsensors, systems and devices for high-temperature and harsh-environment applications, Industrial Electronics, IEEE Transactions on Industrial Electronics 48 (2001) 249–257.

[12] Y. Yuan, C.J. Zhao, X.H. Zhou, B. Tang, S.R. Zhang, High-temperature stable dielectrics in Mn-modified $(1-x)Bi_{0.5}Na_{0.5}TiO_3$–$xCaTiO_3$ ceramics, Journal of Electroceramics 25 (2010) 212–217.

[13] J.B. Lim, S. Zhang, N. Kim, T.R. Shrout, High-temperature dielectrics in the $BiScO_3$–$BaTiO_3$–$(K_{1/2}Bi_{1/2})TiO_3$ ternary system, Journal of the American Ceramic Society 92 (2009) 679–682.

[14] L. Li, D. Guo, W. Xia, Q. Liao, Y. Han, Y. Peng, An ultra-broad working temperature dielectric material of $BaTiO_3$-based ceramics with Nd_2O_3 addition, Journal of the American Ceramic Society 95 (2012) 2107–2109.

[15] J.H. Hwang, S.K. Choi, Y.H. Han, Dielectric properties of $BaTiO_3$ codoped with Er_2O_3 and MgO, Japanese Journal of Applied Physics 40 (2001) 4952.

[16] S. Wang, S. Zhang, X. Zhou, B. Li, Z. Chen, Influence of sintering atmosphere on the microstructure and electrical properties of $BaTiO_3$-based X8R materials, Journal of Materials Science 41 (2006) 1813–1817.

[17] S.H. Yoon, J.H. Lee, D.Y. Kim, N.M. Hwang, Effect of the liquid-phase characteristic on the microstructures and dielectric properties of donor-(niobium) and acceptor-(magnesium) doped barium titanate, Journal of the American Ceramic Society 86 (2003) 88–92.

[18] J.S. Park, M.H. Yang, Y.H. Han, Effects of MgO coating on the sintering behavior and dielectric properties of $BaTiO_3$, Materials Chemistry and Physics 104 (2007) 261–266.

[19] J.S. Park, Y.H. Han, Effects of MgO coating on microstructure and dielectric properties of $BaTiO_3$, Journal of the European Ceramic Society 27 (2007) 1077–1082.

[20] Y. Li, X. Yao, L. Zhang, Dielectric properties and microstructure of magnesium-doped $Ba_{1+k}(Ti_{1-x}Ca_x)O_{3-x+k}$ ceramics, Ceramics International 30 (2004) 1283–1287.

[21] L. Zhang, O.P. Thakur, A. Feteira, G.M. Keith, A.G. Mould, D. C. Sinclair, A.R. West, Comment on the use of calcium as a dopant in X8R $BaTiO_3$-based ceramics, Applied Physics Letters 90 (2007) 142914.

[22] H. Wu, Y. Pu, Z. Wang, K. Chen, Study of electrical and dielectric properties of Y_2O_3 doped $Ba_{1-x}(Bi_{0.5}Na_{0.5})_xTiO_3$ ceramics, Materials Letters 76 (2012) 222–225.

[23] P. Bomlai, N. Sirikulrat, T. Tunkasiri, Effect of heating rate on the properties of Sb and Mn-doped barium strontium titanate PTCR ceramics, Materials Letters 59 (2005) 118–122.

[24] T. Bin, Z. Shu-Ren, Z. Xiao-Hua, Effect of Mn^{2+} doping on the temperature coefficient of capacitance of TiO_2/SiO_2-doped $BaTiO_3$ ceramics, Inorganic Materials 44 (2008) 669–672.

[25] D. Völtzke, H. Abicht, Mechanistic investigations on the densification behaviour of barium titanate ceramics, Solid State Sciences 3 (2001) 417–422.